Author: Satyam Shah

UNIVERSITY OF LEICESTER

GY7711

Field Scientific Report

A field-based report on the application of various geospatial surveying techniques

Student : Satyam Shah

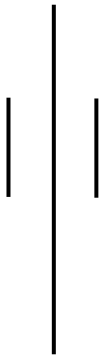

CW2

School of Geography, Geology and the Environment Sciences

University of Leicester

May 2025

Contact: satyamshah444@gmail.com Portfolio: https://satyamspace.github.io/

Table of Contents

1. Introduction

Recent advancements in geospatial surveying have significantly enhanced the ability to capture and analyse physical surroundings with high-levels of accuracy and detail. These developments have had significant impact on various disciplines such as archaeology, urban planning, heritage conservation and environment preservation where reliable spatial inputs are essential to acquire precise outputs in sensitive developmental domains (Walter, 2022). Thus, as such methods become more widely adopted, evaluating their operational performance across various terrain, topography, structural complexity levels and environment circumstances is equally crucial to ensure the reliability of technologies in diverse real-world applications.

This field report documents a comprehensive series of geospatial surveys conducted across multiple sites in and around Leicester from April 28th to May 2nd, 2025. The surveys implemented five different data capture approaches (Terrestrial Laser Scanning (TLS), Structure from Motion, Total Station, and GNSS) along with aerial data acquisition using UAV technology. Each approach was applied in strategically chosen areas to exhibit their respective capabilities. The TLS survey was carried out at Welford Road Cemetery, a Victorian burial ground established in 1849(Leicester city council, 2025). The survey particularly focused on a prominent memorial monument located approximately 50 meters from the main entrance. This monument, among the tallest in the cemetery, was selected due to its intricate geometry, detailed architectural elements and open positioning. The structure's complex surface geometry and vertical reach made it particularly well-suited for testing the laser scanner's performance in capturing point cloud data. (Luhmann et al., 2019) notably suggests, historical monuments pose challenges for 3D documentation due to irregular geometries due to erosion and weathered surfaces, making them suitable test cases for assessing scanner precision.

The Structure from Motion (SfM) was conducted in the northwestern region of Welford Road cemetery, located further from the main entrance. Here, a visually prominent funerary monument with distinctive sculptural elements was chosen. This gravestone consisted intricate carvings, varied textures and complex geometry presenting the site as an ideal subject for photogrammetric reconstruction. The monument position facilitated complete 360-degree access and overhead imaging, allowing comprehensive photographic coverage from multiple angles and elevations which as noted by (Remondino, 2017) is a crucial requirement for SfM processing. According to (Georgopoulos, 2017), close range photogrammetry acquires a sub-millimeter accuracy when capturing cultural heritage objects under-controlled environmental and imaging conditions.

Likewise, the Total Station Survey was carried out in Victoria Park, focusing on tasks centered around the ornamental pond area. The survey covered an area of approximately 0.75 hectares, characterized by gently varying terrain with elevation differences ranging from 1 to 3 meters. The landscape included light sporadic vegetation cover and mown paths for pedestrians. The topographic diversity within a relatively compact area made the site ideal for demonstrating conventional surveying techniques. As emphasized by

(Bangen, 2013), water features often challenge traditional survey methods due to irregular margins, making this approach a valuable inclusion for evaluating capabilities.

The GNSS survey focused on two distinctive buildings at the Campus: the Percy Gee and the Freemen's Common Building. The survey covered an area of roughly 1.2 hectares. The Freemen's Common building with its angular architecture and glass facades, posed challenges for satellite signal reception, primarily due to likelihood of multipath interference. The Drone survey at Borough Hill near Daventry, was conducted in a designated field adjacent to the site entrance covering approximately 2 hectares of the eastern side of the hillfort. The area was chosen due to its open space, minimal obstructions and low hazard-level which made it well-suited for drone operations.

2. Methods

2.1 Total Station Survey

A topographic survey was carried out using Leica TS06+ total station. The equipment was set up via the resection method using 3 known DGPS points, with a 1.475, tripod height. The prism pole was set to 1.5m height in recording 77 elevation points for terrain modelling of the site and 18 planimetric points across two ponds divided by a wooden walk bridge, totalling of about 95 points. The data were exported as CSV, cleaned in Excel and imported into Surfer software to generate a triangulated surface using 2D/3D visualisations. Likewise, the data was also imported into ArcGIS Pro for reprojection and interpolation using Kriging and IDW (0.25m cells) with 0.1m contour intervals.

Figure 1: The two merged images show the total station equipment in action collecting elevation data points via transect method, where one person operates the instrument and another holds the prism pole and walk towards the instrument.

Author: Satyam Shah

e)

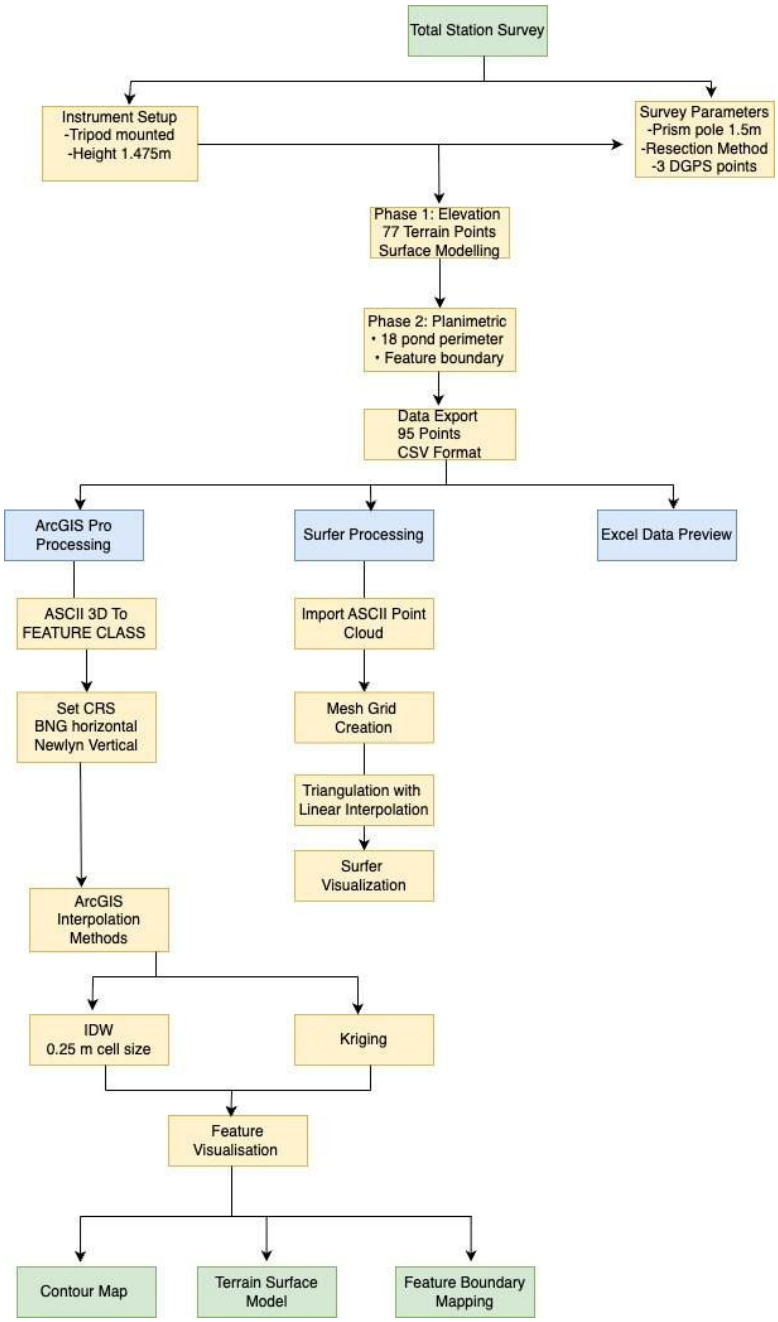

Figure2: Panel (c) shows Pond 1 of the study area and (d) shows Pond 2 ; (e) shows the flowchart and processes carried to generate the results.

Contact: satyamshah444@gmail.com Portfolio: https://satyamspace.github.io/

2.2 GNSS

A high-precision building footprints survey was carried out using Leica GS16/CS20 RTK system in NRTK mode, acquiring centimeter level accuracy. The perimeter points of two buildings: Percy Gee (single perimeter traverse) and Freemen's Common (two circuits for improved average precision). The points were recorded sequentially around parameters of buildings, focusing on corners and linear sections for accurate polygon creation. The data were cleaned in excel and accuracy was assessed in ArcGIS Pro by comparing the GNSS footprints to existing high and low accuracy reference datasets.

Figure 3: The two merged images show the Leica GS16 GNSS instrument being setup for surveying to extract accurate coordinate points.

2.3 Terrestrial Laser Scanning

The Terrestrial Laser Scanning (TLS) was conducted at the Welford Road Cemetery using a Leica P20 to capture high-resolution 3D point cloud data of a tall monument. For this, four registration targets were placed within a 10-meter radius at different heights taking the (ground level, tripod and a nearby monument) into account. The scanner was placed at four fixed positions around the monument maintaining consistent proximity and resolution. The collected scans were imported into Leica's Cyclone software to align using the registered targets, then point clouds were processed in Cloud Compare software to reduce background noise and produce a continuous mesh surface using Poisson surface reconstruction. The mesh was simplified in MeshLab and imported in ArcGIS's ArcScene to georeferenced and scale for integration into the cemetery map.

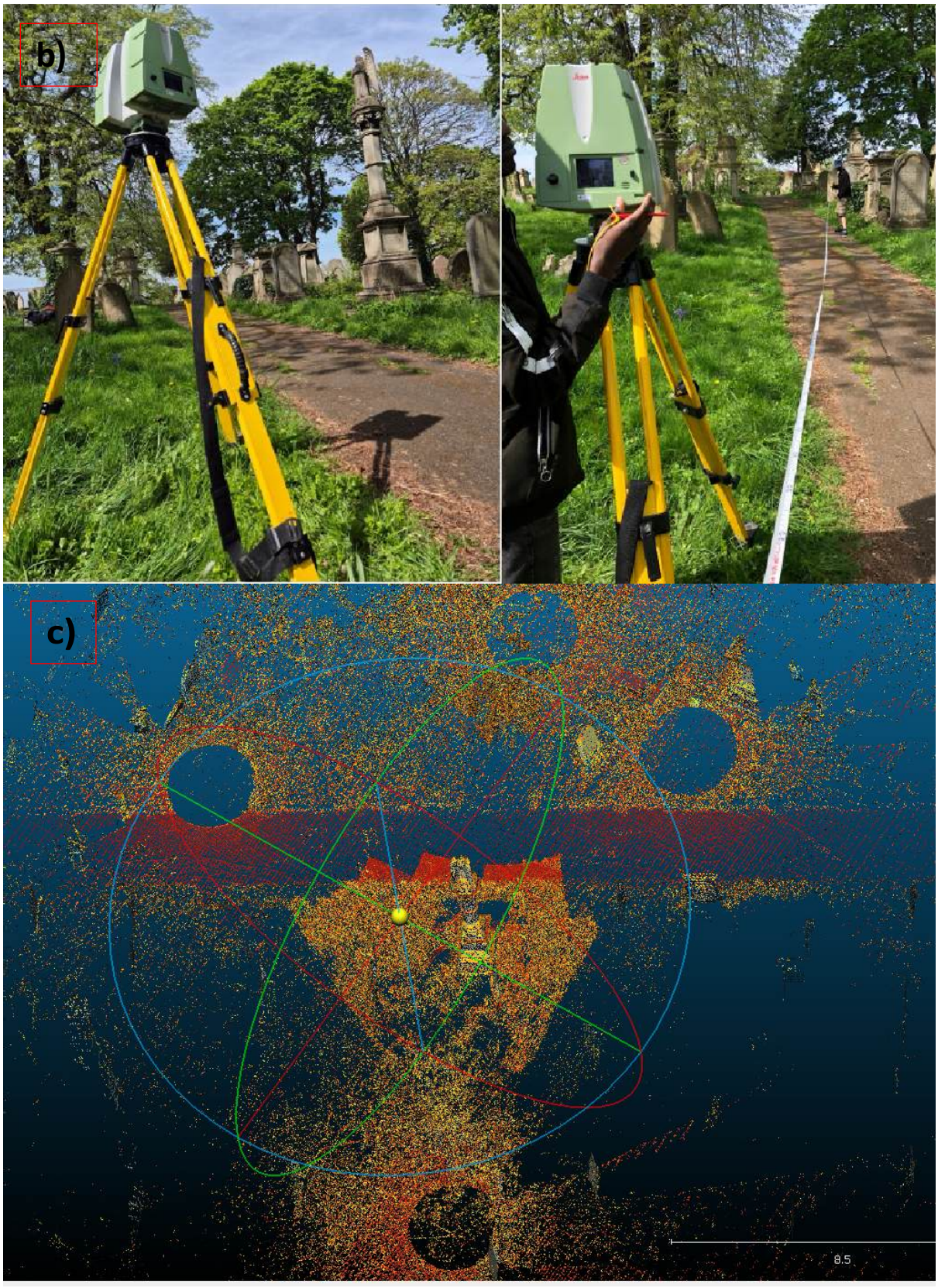

Figure 4: The merged images (a) show the targets being placed around the monument ;(b) show the scanner placed across the monument and distance being measured between the instrument and targets; (c) shows the total 4 locations where the instrument was placed for collecting the data

Author: Satyam Shah

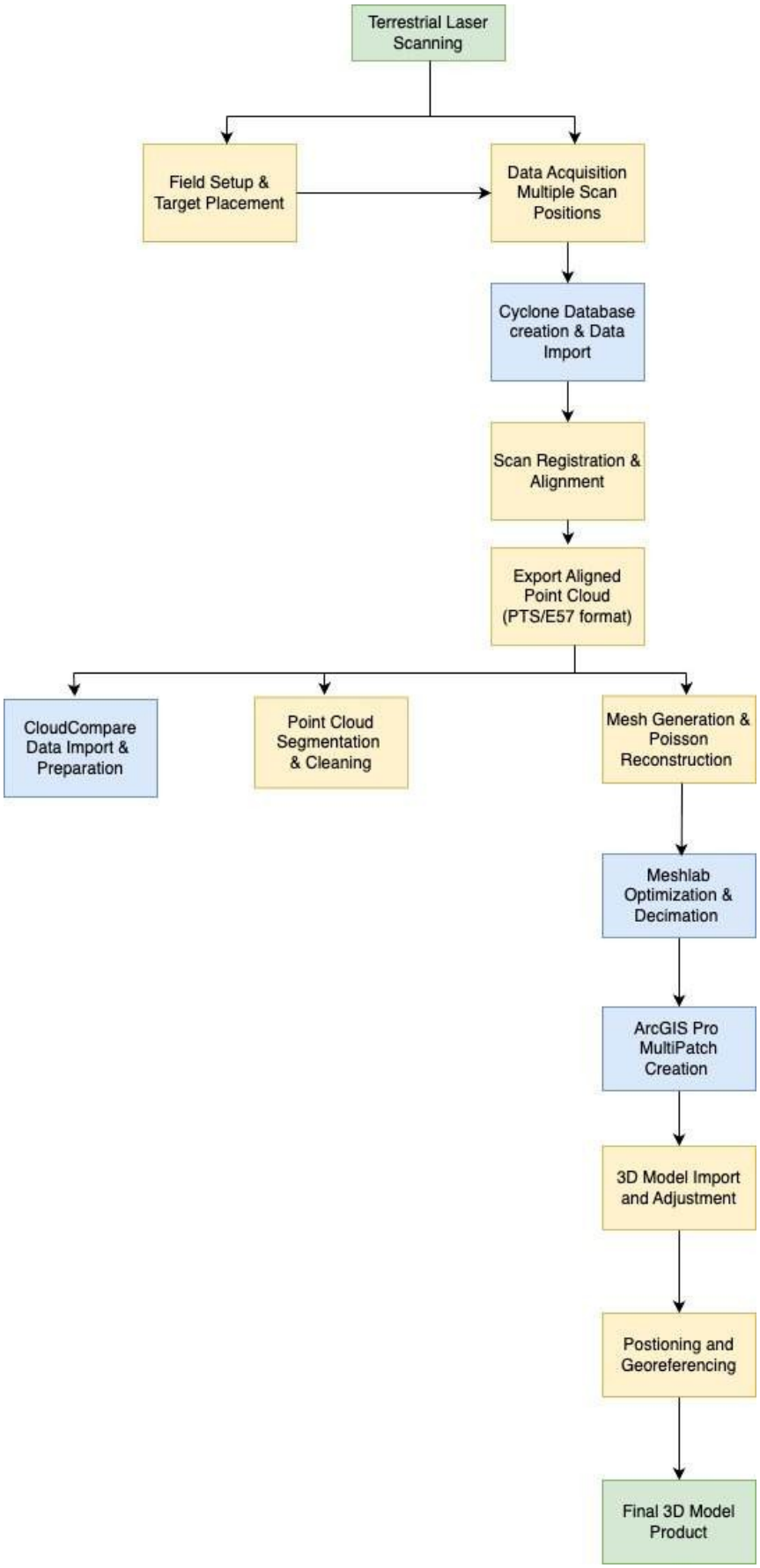

Figure 5: The figure shows the workflow illustrating the data collection and processing steps followed during the survey using Terrestrial Laser Scanner.

2.4 SfM

Structure from Motion (SfM) survey was employed to generate a detailed 3D model of a gravestone. For this, a minimum of 35 photos were taken from an iPhone X systematically from multiple angles (lower, middle, upper) under an overcast light setting, with a tape reference positioned for precise measurements. Then, upon capturing pictures from all heights, a total of 84 pictures were processed in Agisoft Metashape to align and generate a sparse point cloud, followed by dense point cloud construction, texture and mesh generation. The model was exported to MeshLab to scale for real-world dimensions followed by decimation to optimise the size during creation of multipatch feature class in ArcGIS Pro for integrating the 3D scene for spatial visualisation.

Figure 6: The two merged images (a) show the site where the monument is located ; (b) shows the monument being manually assessed prior to SfM photogrammetry using tape measure.

Author: Satyam Shah

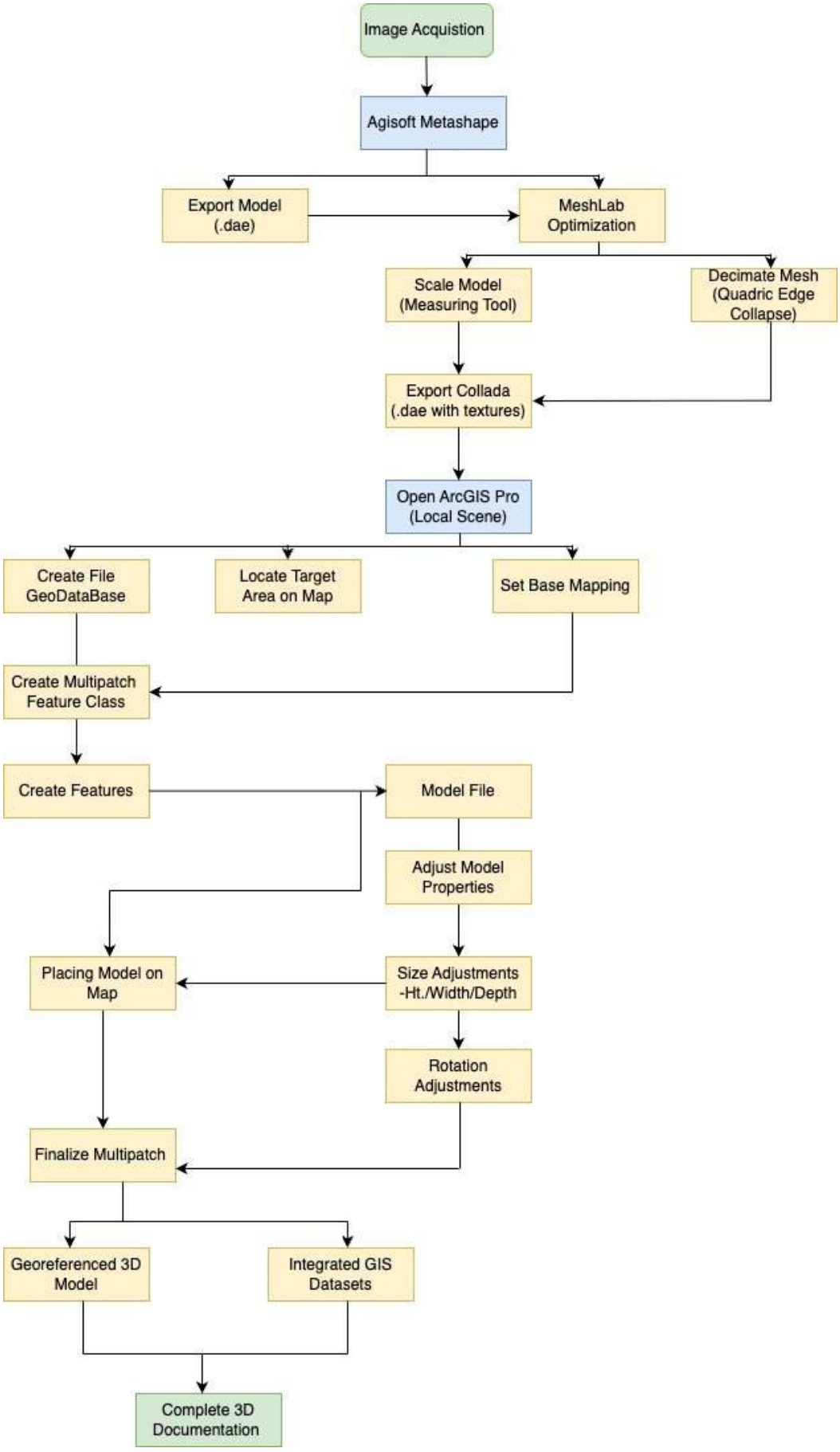

Figure 7: The figure shows the workflow illustrating the processing and data collection steps carried out during survey using SfM method.

2.5 Drone

Drone Survey involved conducting a pre-flight and on-site checklist such as local air traffic, livestock, hazards prior to flying a drone in 120m in height. It involved using DJI Mavic 4 technology consisting of multispectral sensors and a high-resolution camera mounted onboard the drone, facing downward to capture the detailed imagery of the terrain. The drone-based multi-spectral imaging was done by a qualified pilot to ensure safety. The post-flight dataset containing individual band layers were retrieved and processed using ERDAS Imagine to compute and classify indices such as NDVI, GNDVI and NDRE to highlight the variation in vegetation health and other surface characteristics.

Figure 8: The merged images (a) show the DJI Mavic drone being calibrated prior to taking a flight (b) shows the ground transmitter assigning a mission flight path, height and speed to extract the data.

3. Results

3.1 Total Station Survey

The interpolated elevation surfaces exhibit minor yet distinct variation in topography within the pond area. IDW showed two low-lying zones aligning with Pond 1 and Pond 2 while peak over 81.1m south of Pond 1. Kriging generated much smoother surface, finding southeastern area as the highest point. The total site elevation difference was 1.4m.

Author: Satyam Shah

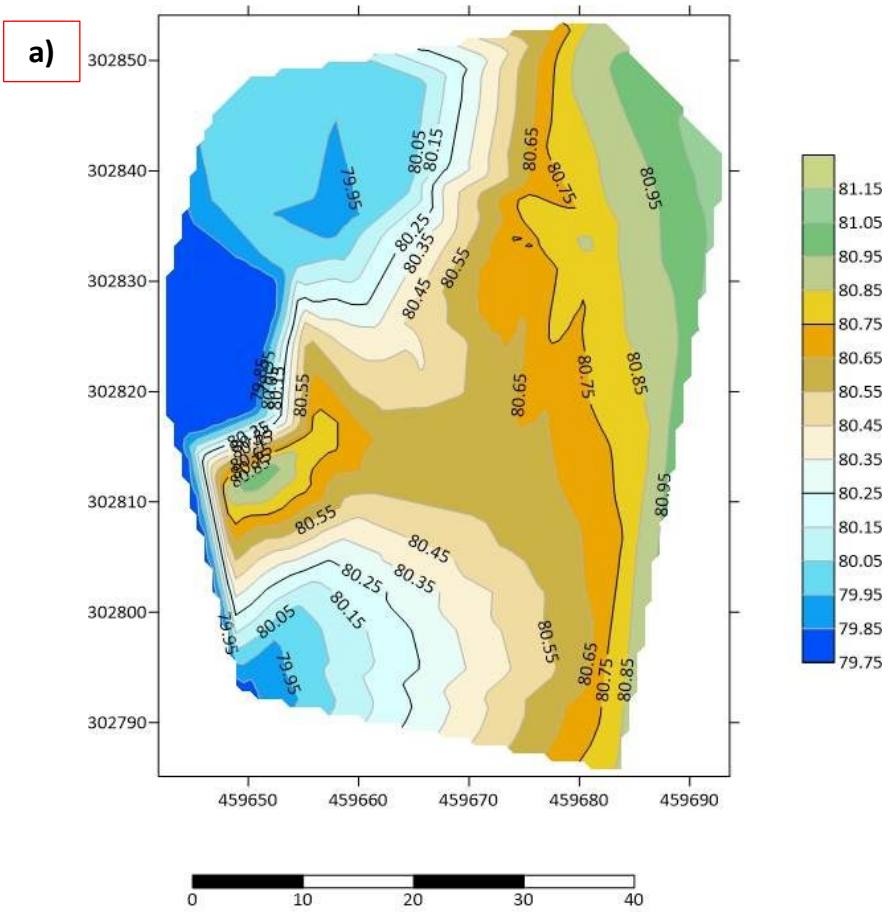

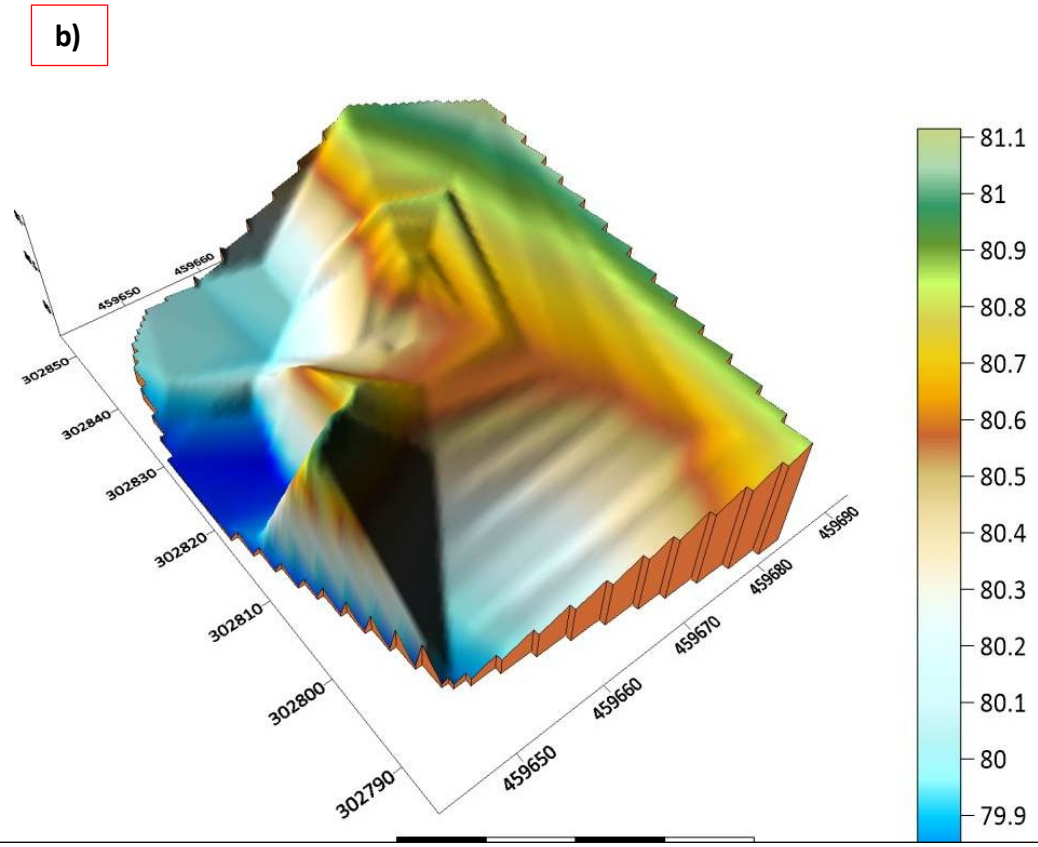

Figure 9: The figure shows topographic contour map (a) showing undulating terrain with highest elevations in the northeast and lowest in the southwest region;(b) shows the 3D surface model of topographic surface revealing surface morphology like steep slope and elevation transition.

c)

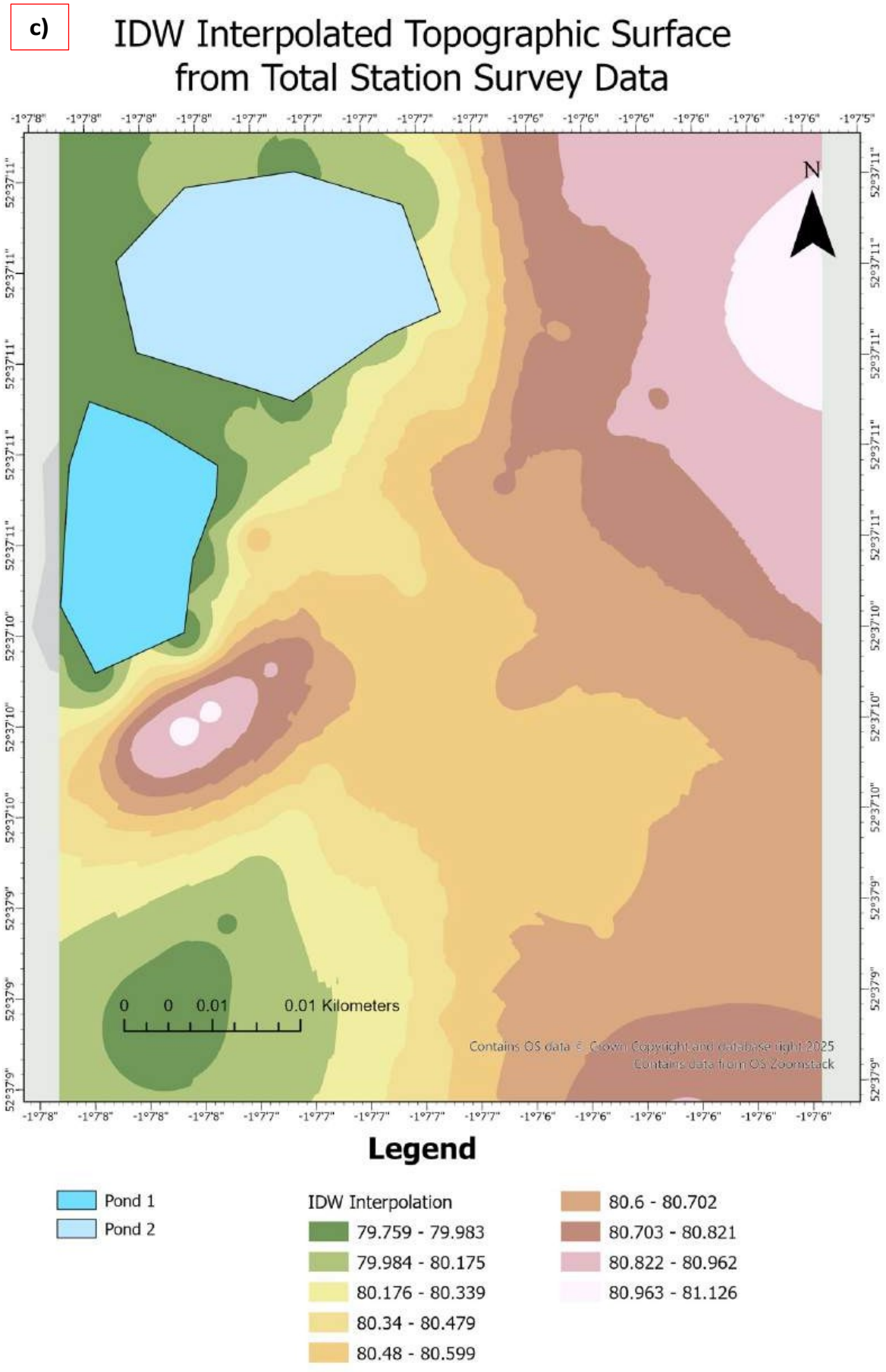

Figure 10: The figure shows the IDW interpolated surface of the study area exhibiting the topographic variability and hydrological features of Pond 1 and Pond 2.

Author: Satyam Shah

d)

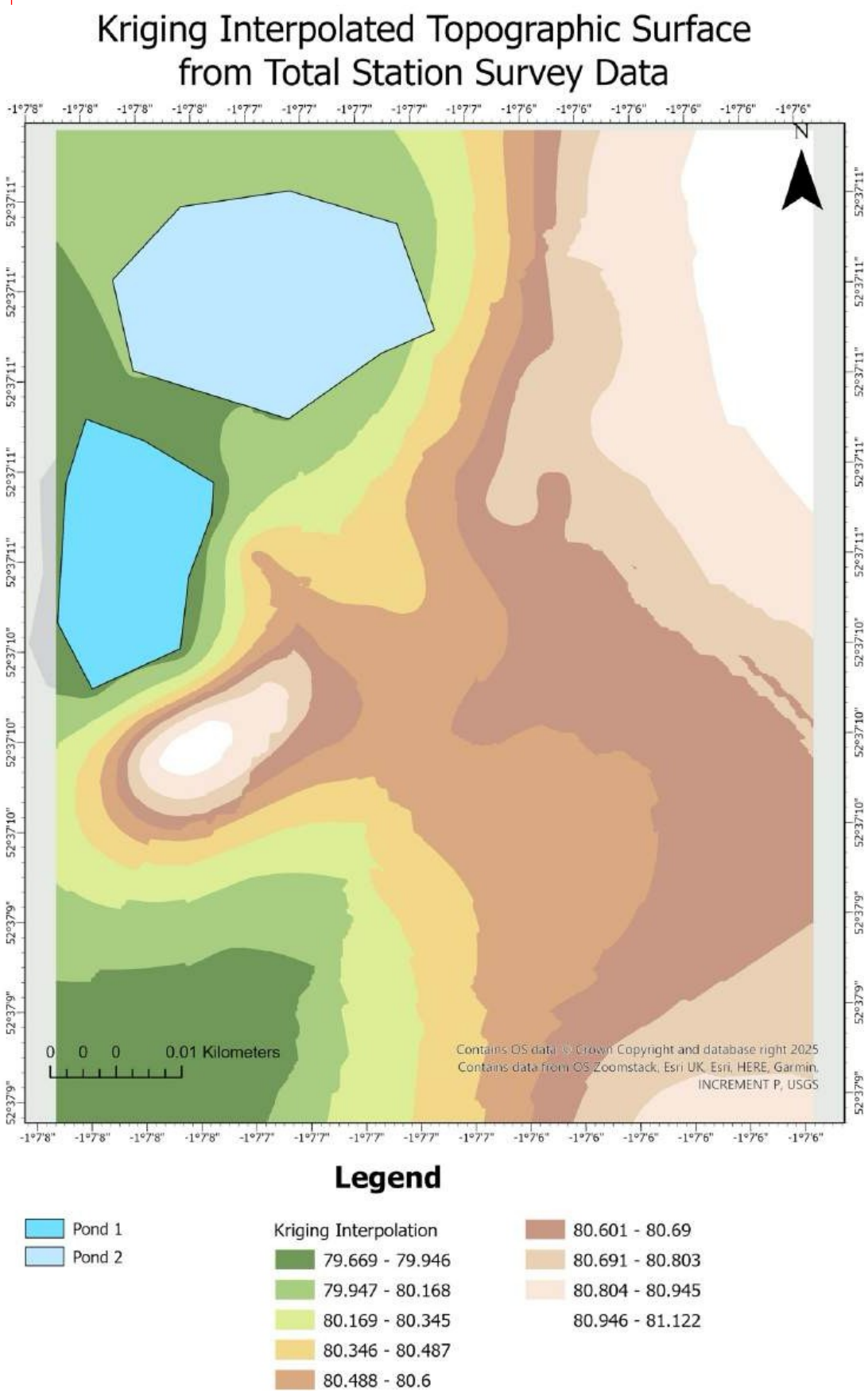

Figure 11: The figure shows the Kriging interpolated surface of the study area exhibiting the topographic variability and hydrological features of Pond 1 and Pond 2.

Contact: satyamshah444@gmail.com Portfolio: https://satyamspace.github.io/

3.2 GNSS

The positional discrepancies between the GNSS recorded points and the high accuracy building footprint ranged from 1.16m to 13.66m. Point 6 was only recorded once resulting in a deviation of 45.65m while Point 5 showed highest variability between trials with distances of 6.46m and 20.86m. Likewise, when compared with the low accuracy dataset, the average deviations ranged from 2.91m(Point 4) to 11.74 (Point5). Notably, points 4 and 7 showed the most consistent results in both reference datasets.

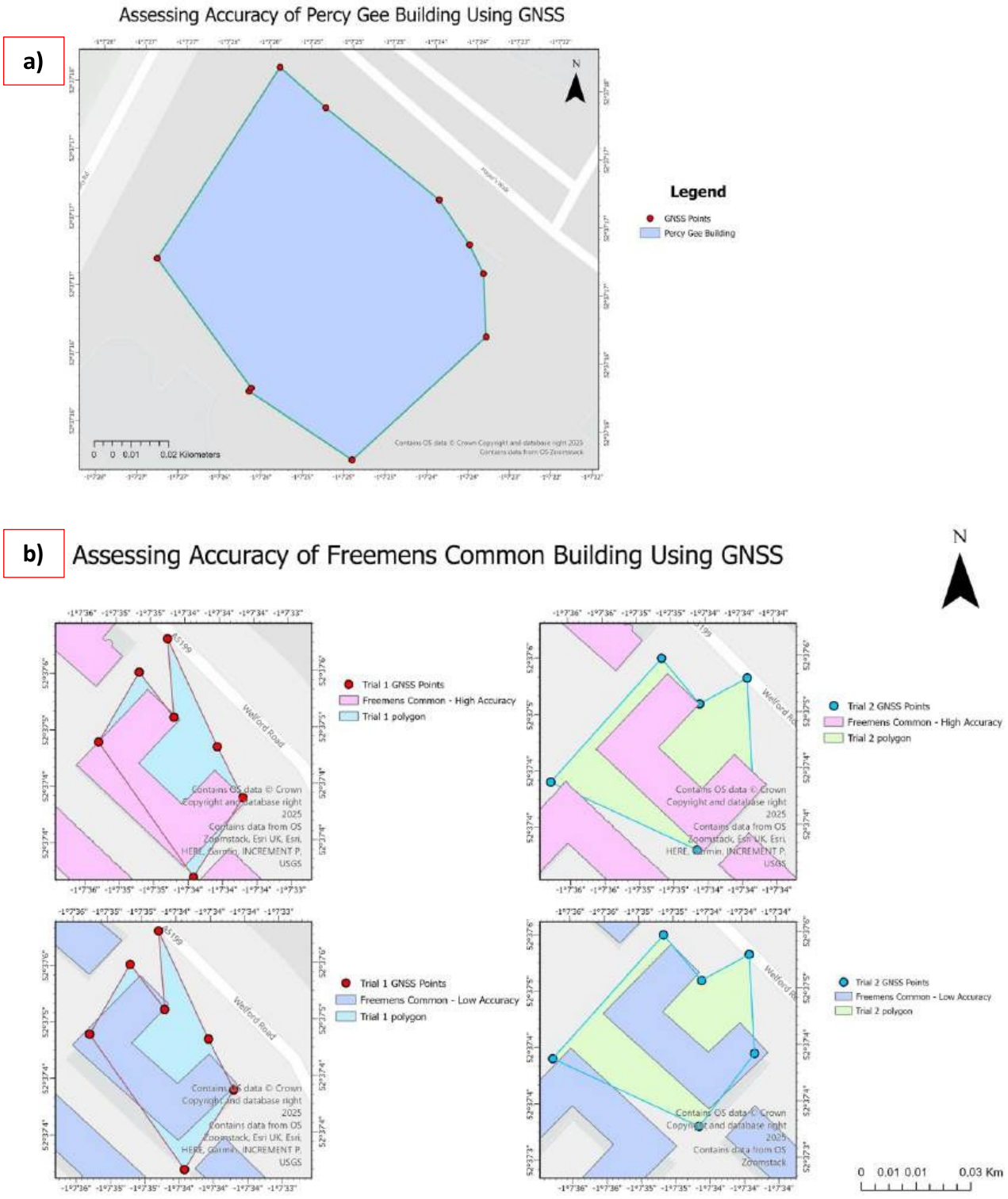

Figure 12: The figure (1) shows the GNSS accuracy of points taken to generate a polygon of Percy Gee building;(b) shows the accuracy of points taken in two trials of Freemens Common and accuracy being compared with low and high accurate building footprints.

3.3 SfM

The photogrammetric reconstruction yielded a high-resolution 3D model of the Victorian funerary monument, capturing intricate details of Gothic architecture with sharp geometric and visual accuracy. It highlights prominent architectural elements like tiered base, Gothic arches, spired pinnacles and carvings. The texture mapping preserved features like weathered stone, lichen patterns and inscriptions. The model's dimensional accuracy was verified to be within ±5mm containing around 2.3 million points. The model also revealed carved foliage and areas of stone decay including hidden elements such as rear panel and internal structural connections.

Figure 13: The figure (a) shows the SfM 3D product of gothic cemetery monument in two different angles;(b) shows the product in 2D angle to get wider context of the model.

3.4 TLS

The TLS survey generated a detailed 3D model as observed in Figure 14, the model accurately showed a high-resolution reconstruction with intricate features such as fluted columns, base contours and the angelic figure at the top of the monument. The process achieved high precision alignment between all four scan positions with a mean absolute error of 2.8mm indicating high geometric consistency. The consistent point density and detailed coverage across all viewpoints indicate the effectiveness of multi-angle scan alignment with minimal disruptions linked to shadowing or occlusion.

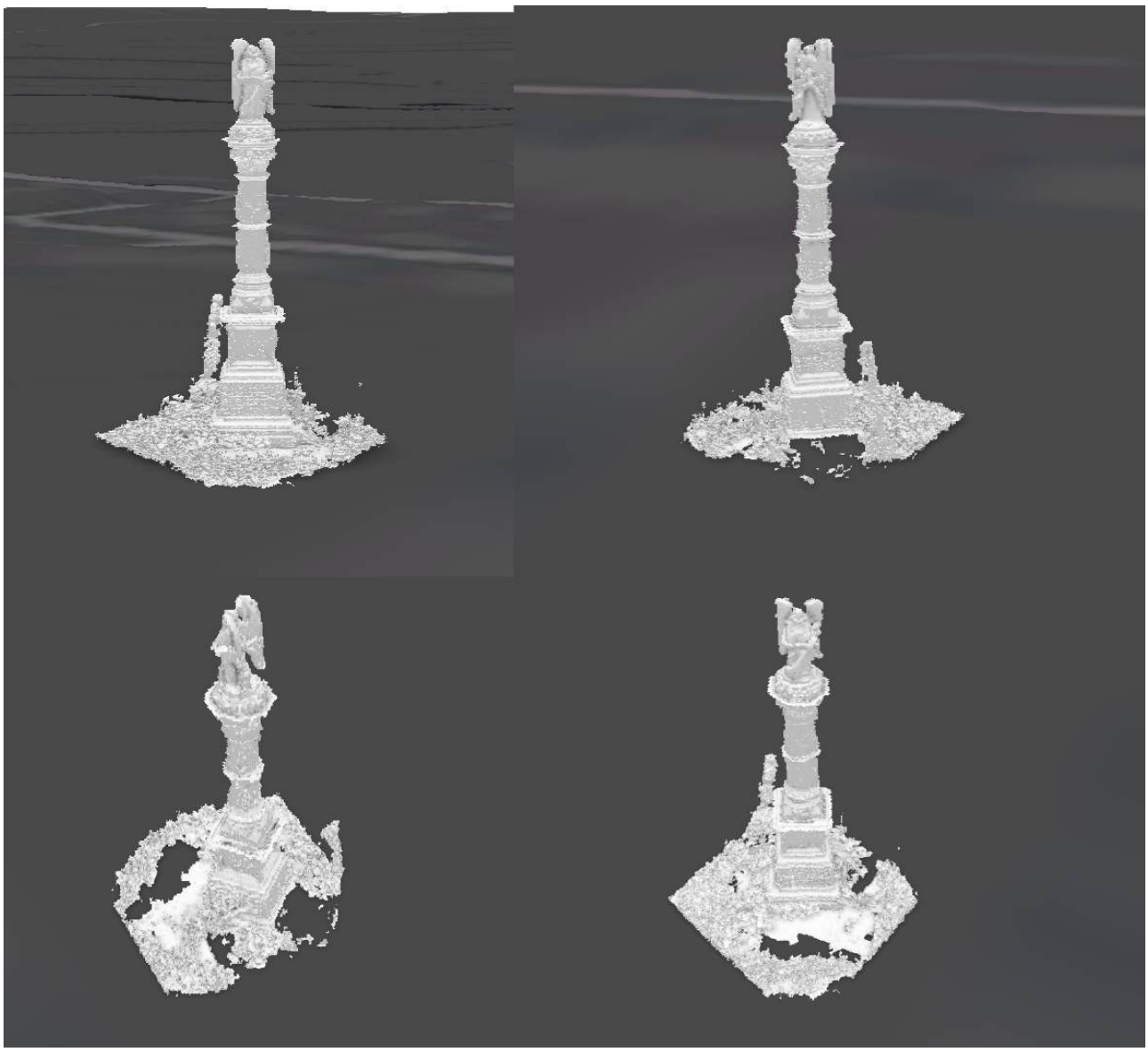

Figure 14: The figure shows the 3D model product generated by the TLS surveying method where the cemetery monument can be observed from four different angles and perspectives.

3.5 Drone

The drone survey derived outputs provided detailed vegetation and surface condition assessments. NDVI ranged from -0.80 to 0.54, with a mean of 0.19 (±0.14 standard deviation) revealing clear patterns of vegetation cover across the study area where areas of healthy vegetation showed highest NDVI values appearing green, whereas moderate vegetation areas showed values between 0.20-0.45 with yellow-green tones, while bare soil zones showed values between 0.0-0.20 as red/orange. The lowest values, down to -0.80 indicated shadowed or non-vegetated surfaces.

NDRE values ranged from -0.58 to 0.45, with a mean of -0.01 (±0.08), revealing a near-even distribution between healthy and stressed vegetation across the study area. Higher NDRE values (0.35-0.45) pointed healthy plants with ample nitrogen level, while moderate scores (0.0-0.35) suggested varying nitrogen levels. Negative values (-0.58 to 0.0) indicated stressed vegetation.

GNDVI showed an average near zero, indicating generally low to moderate photosynthetic activity. High GNDVI (0.50-0.75) were associated with high photosynthetic activity, found in darker green regions. Moderate values (0.0-0.50) indicated variable plant health, while negative values (-0.43 to 0.0) corresponded to areas with little vegetation or non-photosynthetic surfaces.

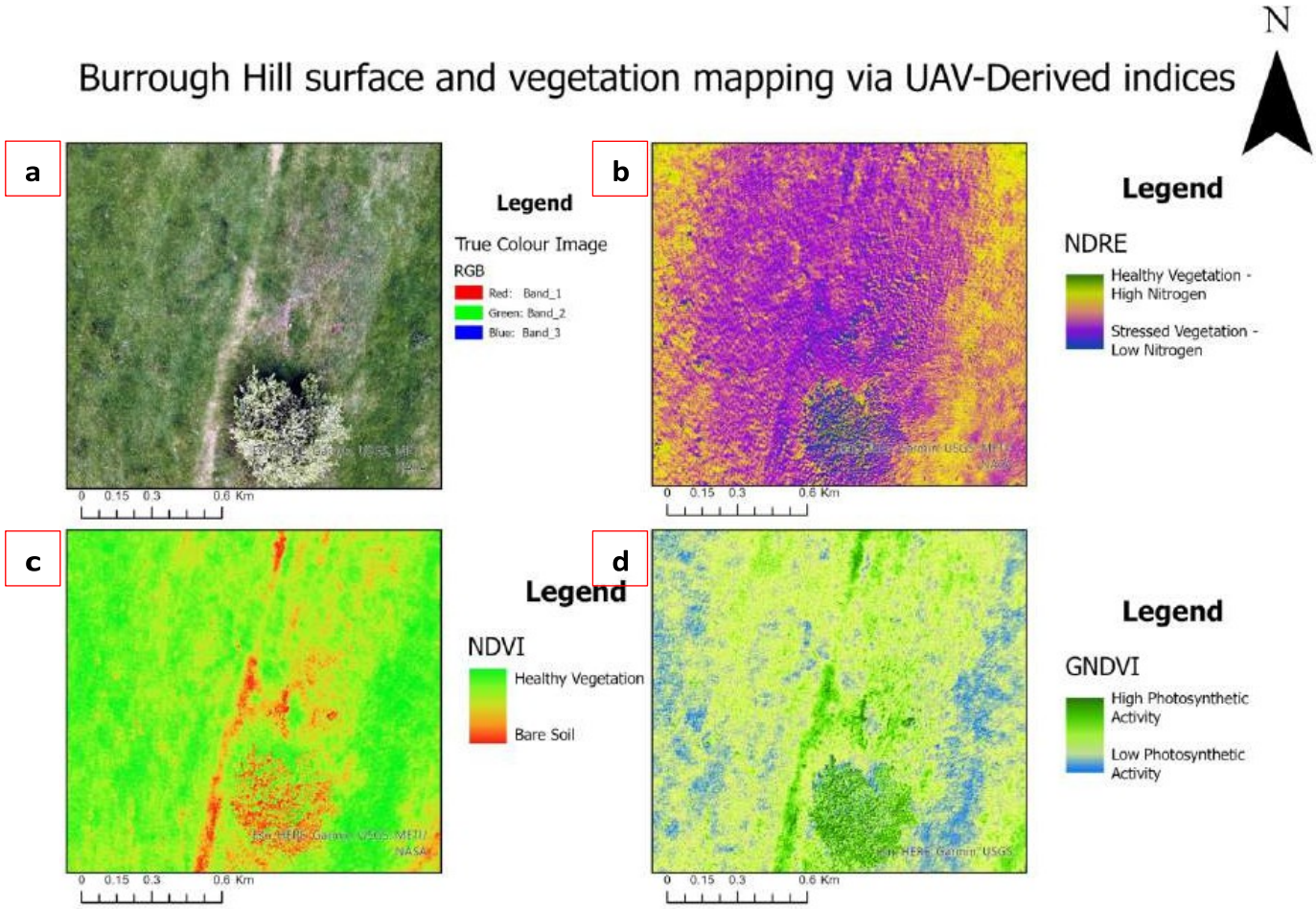

Figure 15: The figure shows the comparative analysis of vegetation indices (a) True Colour Composite;(b) shows NDRE;(c) NDVI and (d) shows GNDVI derived from UAV imagery at Burrough Hill.

4. Discussion

4.1 Total Station

The topographic surfaces generated from the survey provide critical information into the pond system's morphology. Although the observed site's elevation range was 1.4m appearing to be small, such subtle microtopographic variations are vital in constructed wetlands, as even minor changes significantly affect water retention and distribution patterns (Smith et al., 2015). The IDW interpolation identified Pond 1 and Pond 2 as depressions, reflecting wetland morphology. One notable topographic high (81.1m) south of Pond 1 likely indicates residual remnants from recent site modifications between the year 2021-2022. In contrast, the Kriging interpolation provided a smoother view of broader terrain patterns relevant to hydrological function. Moreover, the consistent identification of the southeastern region as the highest terrain by both interpolation approaches, indicates potential areas of undisturbed ground, corroborating the effectiveness of these techniques in environmental monitoring. These similar distinctions align with findings from (Beshr, 2022) who found that IDW excels in delineating detailed features, whereas Kriging is more appropriate for capturing gradual spatial patterns.

4.2 GNSS

The accuracy assessment of building footprints at Freemen's Common provided vital information into the limitations of surveying in urban environments. When applying accuracy assessment framework proposed by (Fan et al., 2014), the positional accuracy determined by calculating the distance between GNSS points and reference footprints deviated substantially from the RTK GNSS system. Although the system possess centimeter-level precision (Aponte et al., 2009), the discrepancies were observed ranging from 1.16m to 13.66m against high and low-accuracy reference data. One notable inconsistency at identical points reveals considerable positional instability supported by (Groom, 2010) findings on multipath interference in urban environments. The shape accuracy via visual comparison of generated polygons against reference data, indicated systematic geometric distortions. While it did reveal general building form, the findings showed consistent offset patterns reflecting (Brovelli and Zamboni's 2018) outcome regarding shape fidelity in urban areas. The completeness evaluation was limited by point collection strategy with varying positional accuracy across trials, suggesting the need for robust sampling methods, such as the building overlap analysis proposed by (Hecht et al., 2013). The GNSS receiver occasionally lost its RTK connection, and it downgraded to a less precise float connection which was standalone positioning when satellite signals were absent. These drops in solution quality reducing accuracy from centimeters to several meters were most common near tall buildings, where poor satellite geometry and signal obstructions were frequent. This fluctuation between positioning modes likely led to inconsistencies across trials and helps explain why points showed large deviations in accuracy from the reference data.

4.3) Comparison of data products

4.3.1) Scale and Accuracy

All five surveying methods utilised in the field study demonstrated distinct features regarding scale and accuracy and suitability for specific applications.

The Total Station survey achieved centimeter-level precision with 127 elevation points across a 1.4m vertical range, making it highly ideal for topographical mapping. (Puttock et al., 2018) suggests that this method offer vertical accuracy within 5.10mm in environmental contexts, reinforcing their status as a reference standard also affirmed by (James et al., 2017). Furthermore, (Smith et al., 2015) demonstrated that even with 100-150 points per hectare, these surveys yield meaningful hydrological features using strategic sampling as demonstrated with the pond survey outcomes. The spatial interpolations using IDW, Kriging and Triangulated linear interpolation captured local variations and elevation trends, demonstrating the method's adaptability for multi-scale analysis.

Conversely, the GNSS survey showed substantial variability in accuracy with positional deviations ranging from 1.16m to 45.65m compared to reference data. (Dabove and Manzino 2014) observed similar error amplification near tall buildings, with errors escalating from centimetres to several meters. The findings corroborate outcomes by (Kaartinen et al., 2012) quantified horizontal deviation from 0.2m in open areas to over 40m findings indicated that GNSS accuracy can degrade in urban environments due to multipath interference from surrounding structures. A study by (Wang et al., 2018) also attribute this to multipath effects, where reflected signals result positional drift when satellite geometry is compromised linking with the observed inter-trial inconsistencies.

The TLS obtained accurate spatial model in documenting the cemetery monument. The 3D model captured intricate architectural details like column fluting, sculptural elements aligning with (Alshawabkeh et al., 2020) findings, who noted TLS achieve 2-5mm accuracy consistent with the visual assessment. (Lague et al., 2013) also validated sub-centimeter capability on irregular surfaces while (Grussenmeyer et al., 2008) validated TLS superiority for detailed documentation of complex heritage structures, emphasizing that detailed architectural elements necessitate point spacing below 5mm, a criterion achieved by our point clouds.

While SfM showed accuracy comparable to TLS, with accuracy within ±5mm. (Koutsoudis et al., 2014) reported similar outcomes using high-overlap photography. Another study by (Sapirsten, 2016) recorded mean errors of 3-6mm using 60-80 images, closely aligning with our methodology of 75 images. Additionally, (Murtiyoso and Grussenmeyer, 2017) confirmed that optimal SfM reconstructions typically acquire 1-3 million points for monument scale surveys, also aligning with our 2.3-million-point model.

The UAV-multispectral survey focused on radiometric accuracy for vegetation analysis. A study by (Deng et al., 2018) observed that calibrated UAV sensors achieve reflectance accuracy within ±5% of ground truth. (Aasen et al., 2018) also reported NDVI values typically within ±0.08 of ground measurements, supporting the pattern consistency observed in the findings. (Castro et al., 2020) emphasized that calibrated multispectral sensors show high internal consistency, even when absolute values deviate from ground measurements, matching our three vegetation index outputs.

4.3.2) Ease of Generation

The practical workflows associated with each method varied considerably across the methods in field efficiency and processing demands. Total station surveying required field time for 95 points, aligning with (Kingsland, 2020), who documented collection rates of 25-75 points per hour, depending on the nature of terrain. Similarly, (Schutz 2016) found that while fieldwork is time-intensive, the post-processing phase is efficient. (Castagnetti et al., 2013) affirmed that standard software and limited technical expertise suffice for data transformation.

The GNSS method, while theoretically faster, necessitated significant field adjustments within the urban settings. (Montenbruck et al., 2017) found that urban observation times in such environment extent from seconds to minutes. (Garrido et al., 2011) also reported a 60%-80% drop in efficiency in urban corridors, while (Stepniak et al., 2020) stressed the need for repeated recordings and real-time quality checks, consistent with our multi-trial approach. Nonetheless, GNSS required minimal post-processing, supporting the observation of Garrido regarding direct GIS integration.

TLS emerged as the most technically demanding approach. (Grussenmeyer et al., 2008) reported that based on the size and quality of monument, the generation of mode involves 4-8 scanning positions, generating tens of millions of points. (Ramos and Remondino ,2015) stated the post-processing phase to consume upto 10 times the field duration, mainly during registration and filtering. These studies closely align with the output 3D model recorded from 4 scanning positions in medium-quality for quicker processing.

SfM findings demonstrated a balance of field efficiency and data richness. (Sapirstein 2016) found that Sfm surveys only take about 20-25% of the time required for TLS surveys. However, studies suggest that processing high quality images in high number take longer time. (Murtiyoso and Grussenmeyer 2017) emphasized that while modern SfM software is user friendly, obtaining optimal results requires careful parameter tuning.

The UAV survey showed positive efficiency for large area coverage. As per (Tmusic et al., 2020) findings, UAVs survey 5-20 hectares per hour, exceeding ground-based methods. (Singh and Frazier, 2018) reported that this benefit is offset by complex pre-flight planning and regulatory compliance. While the data is comparably easy to generate given UAV operate in its optimal condition, the storing and processing of high-quality images and mosaicking require extensive technical expertise and cost.

4.3.3) Ease of GIS Integration

The ease of GIS integration capabilities varied across surveys. As per (Puttock et al., 2018) Total station data typically consumed 30 minutes to integrate into the GIS environment. The use of IDW and Kriging interpolation aligned (Smith et al., 2015) findings that such algorithms perform well when point density exceeds 100 points per hectare. Likewise, GNSS data also offered direct integration, although quality control was one limitation. (Junichi, 2014) showed how coordinate system compatibility is one primary GNSS advantage. (Guo et al., 2017) found that visual judgement is often required to ensure topological correctness to fit and align with reference datasets for better integration. TLS data presented significant integration challenges. As per (Ramos and Remondino 2015), point clouds require intensive preprocessing prior to incorporating it into the GIS workflow. Thus, the use of multiple softwares aligns with (Grussenmeyer et al., 2008) findings on interoperability problems. SfM outputs also shared similar integration challenges, although beneficial for visualisation. (Sapirsten, 2016) reported that SfM offers both gemetric and visual data, supporting multiple GIS applications. Thus, the obtained generated textured model aligns with (Koutsoudis et al.,2014) findings on SfM's ability to provide visual documentation. In addition (Murtiyoso, 2017) indicated how modern photogrammetric software increasingly support unprocessed raw data product in exporting to GIS ready formats, thereby reducing technical barriers. The UAV-derived multispectral data was the most GIS-compatible product in terms of accuracy that automatically aligned with GIS structure with minimal processing. (Sofonia et al., 2019) also emphasized how calibrated index products support basic GIS analyses without use of extensive GIS tech stack and transformation techniques.

References

Alshawabkeh, Y., El-Khalili, M., Almasri, E., Bala'awi, F. and Al-Massarweh, A. (2020). Heritage documentation using laser scanner and photogrammetry. The case study of Qasr Al-Abidit, Jordan. Digital Applications in Archaeology and Cultural Heritage, 16, p.e00133. doi: https://doi.org/10.1016/j.daach.2019.e00133.

Aponte, J.D., Meng, X., Hill, C., Moore, T., Burbidge, M. and Dodson, A. (2009). Quality assessment of a network-based RTK GPS service in the UK. 3(1). doi:https://doi.org/10.1515/jag.2009.003.

Ashraf and Kaloop, M.R. (2022). Using modified inverse distance weight and principal component analysis for spatial interpolation of foundation settlement based on geodetic observations. Open Geosciences, 14(1), pp.1310–1323. doi:https://doi.org/10.1515/geo-2022-0402.

Bangen, S.G. (2013). Comparison of topographic surveying techniques in streams. doi:https://doi.org/10.26076/7e1e-3c6f.

Brovelli, M. and Zamboni, G. (2018). A New Method for the Assessment of Spatial Accuracy and Completeness of OpenStreetMap Building Footprints. ISPRS International Journal of Geo-Information, 7(8), p.289. doi:https://doi.org/10.3390/ijgi7080289.

Castagnetti, C., Bertacchini, E., Corsini, A. and Capra, A. (2013). Multi-sensors integrated system for landslide monitoring: critical issues in system setup and data management. European Journal of Remote Sensing, 46(1), pp.104–124. doi:https://doi.org/10.5721/eujrs20134607.

Dabove, P. and Manzino, A. (2014). GPS C GLONASS Mass-Market Receivers: Positioning Performances and Peculiarities. Sensors, 14(12), pp.22159–22179. doi:https://doi.org/10.3390/s141222159.

De Vries, W.T. (2022). Trends in The Adoption of New Geospatial Technologies for Spatial Planning and Land Management in 2021. Geoplanning: Journal of Geomatics and Planning, 8(2), pp.85–98. doi:https://doi.org/10.14710/geoplanning.8.2.85-98.

Deng, L., Mao, Z., Li, X., Hu, Z., Duan, F. and Yan, Y. (2018). UAV-based multispectral remote sensing for precision agriculture: A comparison between different cameras. ISPRS Journal of Photogrammetry and Remote Sensing, 146, pp.124–136. doi:https://doi.org/10.1016/j.isprsjprs.2018.09.008.

Fabio Remondino, Nocerino, E., Toschi, I. and Menna, F. (2017). A CRITICAL REVIEW OF AUTOMATED PHOTOGRAMMETRIC PROCESSING OF LARGE DATASETS. The International Archives of the Photogrammetry, Remote Sensing and Spatial Information Sciences, XLII-2/W5, pp.591–599. doi:https://doi.org/10.5194/isprs-archives-xlii-2-w5-591-2017.

Fan, H., Zipf, A., Fu, Q. and Neis, P. (2014). Quality assessment for building footprints data on OpenStreetMap. International Journal of Geographical Information Science, 28(4), pp.700–719. doi:https://doi.org/10.1080/13658816.2013.867495.

Fonte, C. C., Antoniou, V., Bastin, L., Estima, J., Arsanjani, J. J., Bayas, J-C. L., See, L. and Vatseva, R. (2017) Assessing VGI Data Quality. In: Foody, G., See, L., Fritz, S., Mooney, P., Olteanu-Raimond, A-M., Fonte, C. C. and Antoniou, V. (eds.) Mapping and the Citizen Sensor. pp. 137–163. London: Ubiquity Press. DOI: https://doi.org/10.5334/bbf.g License: CC-BY 4.0

Garrido, M.S., Giménez, E., Clara and Gil, A.J. (2011). Testing precise positioning using RTK and NRTK corrections provided by MAC and VRS approaches in SE Spain. Journal of Spatial Science, 56(2), pp.169–184. doi:https://doi.org/10.1080/14498596.2011.623341.

Georgopoulos, A. and Stathopoulou, E.K. (2017). Data Acquisition for 3D Geometric Recording: State of the Art and Recent Innovations. Quantitative methods in the humanities and social sciences, pp.1–26. doi:https://doi.org/10.1007/978-3-319-65370-9_1.

Groom, R. (2010) Guidelines for the use of GNSS in land surveying and mapping: RICS guidance note. 2nd ed. Coventry: RICS. Available at: https://www.rics.org/profession-standards/rics-standards-and-guidance/sector-standards/land-standards/guidelines-for-the-use-of-gnss-in-land-surveying-and-mapping

Grussenmeyer, P., Landes, T., Voegtle, T. and Ringle, K., 2008. Comparison methods of terrestrial laser scanning, photogrammetry and tacheometry data for recording of cultural heritage buildings. International Archives of Photogrammetry, Remote Sensing and Spatial Information Sciences, 37(B5), pp.213-218.

Guo, J., Li, X., Chen, X., Geng, J., Wen, Q. and Pan, Y. (2017). Performance Analysis of Multi-GNSS Precise Point Positioning. Lecture notes in electrical engineering, pp.377–387. doi:https://doi.org/10.1007/978-981-10-4594-3_32.

Hecht, R., Kunze, C. and Hahmann, S. (2013). Measuring Completeness of Building Footprints in OpenStreetMap over Space and Time. ISPRS International Journal of Geo-Information, 2(4), pp.1066–1091. doi:https://doi.org/10.3390/ijgi2041066.

James, M.R., Robson, S., d'Oleire-Oltmanns, S. and Niethammer, U. (2017). Optimising UAV topographic surveys processed with structure-from-motion: Ground control quality, quantity and bundle adjustment. Geomorphology, 280, pp.51–66. doi:https://doi.org/10.1016/j.geomorph.2016.11.021.

Junichi SUSAKI (2014). AUTOMATIC EXTRACTION OF BUILDINGS IN DENSE URBAN AREAS USING AERIAL IMAGES AND AIRBORNE LIDAR DATA. Journal of Japan Society of Civil Engineers Ser F3 (Civil Engineering Informatics), 70(2), pp.I_123–I_132. doi:https://doi.org/10.2208/jscejcei.70.i_123.

Kaartinen, H., Hyyppä, J., Kukko, A., Jaakkola, A. and Hyyppä, H. (2012). Benchmarking the Performance of Mobile Laser Scanning Systems Using a Permanent Test Field. Sensors, 12(9), pp.12814–12835. doi:https://doi.org/10.3390/s120912814.

Karstens, S., Jurasinski, G., Glatzel, S. and Buczko, U. (2016). Dynamics of surface elevation and microtopography in different zones of a coastal Phragmites wetland. Ecological Engineering, 94, pp.152–163. doi:https://doi.org/10.1016/j.ecoleng.2016.05.049.

Kingsland, K. (2020). Comparative analysis of digital photogrammetry software for cultural heritage. Digital Applications in Archaeology and Cultural Heritage, 18, p.e00157. doi:https://doi.org/10.1016/j.daach.2020.e00157.

Koutsoudis, A., Vidmar, B., Ioannakis, G., Arnaoutoglou, F., Pavlidis, G. and Chamzas, C. (2014). Multi-image 3D reconstruction data evaluation. Journal of Cultural Heritage, [online] 15(1), pp.73–79. doi:https://doi.org/10.1016/j.culher.2012.12.003.

Lague, D., Brodu, N. and Leroux, J. (2013). Accurate 3D comparison of complex topography with terrestrial laser scanner: Application to the Rangitikei canyon (N-Z).

ISPRS Journal of Photogrammetry and Remote Sensing, 82, pp.10–26. doi:https://doi.org/10.1016/j.isprsjprs.2013.04.009.

Luhmann, T., Chizhova, M., Gorkovchuk, D., Hastedt, H., Chachava, N. and Lekveishvili, N. (2019). COMBINATION OF TERRESTRIAL LASERSCANNING, UAV AND CLOSE-RANGE PHOTOGRAMMETRY FOR 3D RECONSTRUCTION OF COMPLEX CHURCHES IN GEORGIA. The International Archives of the Photogrammetry, Remote Sensing and Spatial Information Sciences, XLII-2/W11, pp.753–761. doi:https://doi.org/10.5194/isprs-archives-xlii-2-w11-753-2019.

Lynch, J.C., Winn, N., Kovalenko, K. and Guntenspergen, G. (2023). Comparing Wetland Elevation Change Using a Surface Elevation Table, Digital Level, and Total Station. Estuaries and Coasts. doi:https://doi.org/10.1007/s12237-023-01263-1.

Montenbruck, O., Steigenberger, P., Prange, L., Deng, Z., Zhao, Q., Perosanz, F., Romero, I., Noll, C., Stürze, A., Weber, G., Schmid, R., MacLeod, K. and Schaer, S. (2017). The Multi-GNSS Experiment (MGEX) of the International GNSS Service (IGS) – Achievements, prospects and challenges. Advances in Space Research, 59(7), pp.1671–1697. doi:https://doi.org/10.1016/j.asr.2017.01.011.

Moser, K., Ahn, C. and Noe, G. (2007). Characterization of microtopography and its influence on vegetation patterns in created wetlands. Wetlands, 27(4), pp.1081–1097. doi:https://doi.org/10.1672/0277-5212(2007)27[1081:comaii]2.0.co;2.

Murtiyoso, A. and Grussenmeyer, P. (2017). Documentation of heritage buildings using close-range UAV images: dense matching issues, comparison and case studies. The Photogrammetric Record, 32(159), pp.206–229. doi:https://doi.org/10.1111/phor.12197.

Puttock, A.K., Cunliffe, A.M., Anderson, K. and Brazier, R.E. (2015). Aerial photography collected with a multirotor drone reveals impact of Eurasian beaver reintroduction on ecosystem structure. Journal of Unmanned Vehicle Systems, 3(3), pp.123–130. doi:https://doi.org/10.1139/juvs-2015-0005.

Ramos, M.M. and Fabio Remondino (2015). Data fusion in Cultural Heritage – A Review. The International Archives of the Photogrammetry, Remote Sensing and Spatial Information Sciences, XL-5/W7, pp.359–363. doi:https://doi.org/10.5194/isprsarchives-xl-5-w7-359-2015.

Sapirstein, P. (2016). Accurate measurement with photogrammetry at large sites. Journal of Archaeological Science, 66, pp.137–145. doi:https://doi.org/10.1016/j.jas.2016.01.002.

Schütz, M. (2016). Potree: Rendering large point clouds in web browsers. Master's thesis, Vienna University of Technology. https://www.researchgate.net/publication/309358171_Potree_Rendering_Large_Point_Clouds_in_Web_Browsers

Singh, K.K. and Frazier, A.E. (2018). A meta-analysis and review of unmanned aircraft system (UAS) imagery for terrestrial applications. International Journal of Remote Sensing, 39(15-16), pp.5078–5098. doi:https://doi.org/10.1080/01431161.2017.1420941.

Smith, M.W., Carrivick, J.L. and Quincey, D.J. (2015). Structure from motion photogrammetry in physical geography. Progress in Physical Geography: Earth and Environment, 40(2), pp.247–275. doi:https://doi.org/10.1177/0309133315615805.

Sofonia, J., Shendryk, Y., Phinn, S., Roelfsema, C., Kendoul, F. and Skocaj, D. (2019). Monitoring sugarcane growth response to varying nitrogen application rates: A comparison of UAV SLAM LiDAR and photogrammetry. International Journal of Applied Earth Observation and Geoinformation, 82, p.101878. doi:https://doi.org/10.1016/j.jag.2019.05.011.

Su, J. and Bork, E.W. (2006). Influence of Vegetation, Slope, and Lidar Sampling Angle on DEM Accuracy. Photogrammetric Engineering and Remote Sensing, 72(11), pp.1265–1274. doi:https://doi.org/10.7939/r3571821w.

Tmušić, G., Manfreda, S., Aasen, H., James, M.R., Gonçalves, G., Ben-Dor, E., Brook, A., Polinova, M., Arranz, J.J., Mészáros, J., Zhuang, R., Johansen, K., Malbeteau, Y., de Lima, I.P., Davids, C., Herban, S. and McCabe, M.F. (2020). Current Practices in UAS-based Environmental Monitoring. Remote Sensing, 12(6), p.1001. doi:https://doi.org/10.3390/rs12061001.

Wang, L., Li, Z., Ge, M., Neitzel, F., Wang, Z. and Yuan, H. (2018). Validation and Assessment of Multi-GNSS Real-Time Precise Point Positioning in Simulated Kinematic Mode Using IGS Real-Time Service. Remote Sensing, 10(2), p.337. doi:https://doi.org/10.3390/rs10020337.

Westoby, M.J., Brasington, J., Glasser, N.F., Hambrey, M.J. and Reynolds, J.M. (2012). 'Structure-from-Motion' photogrammetry: A low-cost, effective tool for geoscience applications. Geomorphology, 179, pp.300–314.